Hindawi
Geofluids
Volume 2019, Article ID 3850148, 16 pages
https://doi.org/10.1155/2019/3850148

Research Article

Geochemical Characterization of Spring Waters in the Crati River Basin, Calabria (Southern Italy)

Simona Gaglioti,[1] Ernesto Infusino,[1] Tommaso Caloiero,[2] Giovanni Callegari,[2] and Ilaria Guagliardi[2]

[1]*University of Calabria-Department of Environmental and Chemical Engineering (DIATIC), 87036 Rende (CS), Italy*
[2]*National Research Council of Italy-Institute for Agricultural and Forest Systems in the Mediterranean (CNR-ISAFOM), 87036 Rende (CS), Italy*

Correspondence should be addressed to Tommaso Caloiero; tommaso.caloiero@isafom.cnr.it

Received 16 May 2018; Revised 19 September 2018; Accepted 18 November 2018; Published 3 February 2019

Academic Editor: Paulo Fonseca

The characterization of the spatial variation of geochemical parameters in spring waters, especially the ones used for drinking purpose, is essential to identify potential risks to humans. In this work, results of a qualitative analysis on 190 samples of spring waters collected in the largest catchment of the Calabria region (southern Italy) are shown. Several physical and chemical parameters were analysed and the Langelier-Ludwig diagram was built to evaluate the hydrochemical facies of the sampled waters. Additionally, the relationships between water temperature and altitude and electric conductivity (EC) and altitude were assessed. Geostatistical methods were used to map the physical and chemical parameters. Results showed a good quality status of the spring waters in the Crati basin, with a predominant Ca-Mg-type hydrochemical facies. Then, a connection between EC and temperature with elevation has been detected in some area of the basin. Finally, the spatial analysis allowed identifying the distribution of the concentration of the several parameters.

1. Introduction

Water is the most essential element for the existence of life on Earth, which is becoming increasingly precious during the last decades. In fact, water quality issues are one of the major challenges that humanity is facing in the twenty-first century considering safe drinking water the basic need for every citizen. About 80% of the diseases in the world and one-third of the deaths in the developing countries are caused by contaminated water [1]. In particular, the groundwater is the main source for drinking purposes, sanitary uses, irrigation, and industrial processes. A good management of this resource is very important especially in some areas such as the Mediterranean basin, which is located in a transition zone between North Africa (arid climate) and central Europe (temperate and rainy climate), which is affected by the interaction between midlatitude and tropical processes and which can be considered as potentially vulnerable to climatic changes [2]. In fact, groundwater quality is getting deteriorated also due to climate changes which cause low rainfall and high evapotranspiration [3]. Groundwater quality in a region largely depends on natural processes, like dissolution and precipitation of minerals, groundwater velocity, quality of recharge waters and interaction with other types of water aquifers, and weathering and catchment erosion [4, 5], and on anthropogenic inputs including urbanization, agricultural, and industrial activities. Among the natural factors, geology of the catchment area, degree of chemical weathering of the various rock types, and inputs from sources other than water-rock interaction play a significant role in controlling the chemistry of the water [6–9]. In the last decades, numerous studies have been published about major ions, trace elements, and potentially harmful elements in the water [10–12], giving information about the possible geological and anthropogenic influences on aquifers [13–20]. In fact, by analysing different physical and chemical parameters it is possible to understand the behaviour of groundwater in relation with the lithologies present in each area. High pH and

EC values characterize waters coming from carbonate aquifer where the long-time contact with limestones, dolostones, gypsum, and anhydrite make them alkaline as well as for those from the siliciclastic rocks (in particular calcium-, magnesium-, or iron-rich reservoirs) which present high capacity of CO_2 mineral trapping [21]. Erosion of rocks (e.g., limestone and dolomite) and minerals (e.g., calcite and magnesite) is the most common source of calcium and magnesium [21]. More precisely, calcium is a widespread refractory lithophile element forming several common minerals including calcite $CaCO_3$, gypsum $CaSO_4{\cdot}2H_2O$, dolomite $CaMg(CO_3)_2$, anhydrite $CaSO_4$, and fluorite CaF_2. Calcium is also widely distributed in other minerals such as feldspar, amphibole, and pyroxene and is often associated with clay minerals such as illite, chlorite, and Ca-montmorillonite. In igneous rocks, calcium is enriched in anorthosite, which is composed predominantly of calcium-rich plagioclase feldspar, and in mafic rocks. However, rocks such as granite and sandstone, and their metamorphic equivalents, have relatively low total CaO contents. Magnesium is a lithophile metallic element and a major constituent of many mineral groups, including silicates, carbonates, sulphates, phosphates, and borates. It forms several important minerals, including magnesite $MgCO_3$, dolomite $CaMg(CO_3)_2$, pyrope garnet $Mg_2Al_2(SiO_4)_3$, and kieserit $MgSO_4{\cdot}H_2O$. It is a major component of many mafic rock-forming minerals, such as olivine, e.g., forsterite Mg_2SiO_4, pyroxene, amphibole, spinel $MgAl_2O_4$, biotite mica, chlorite, serpentine, and talc, and clay minerals, such as montmorillonite, as well as less common mineral groups, such as arsenates, halides, nitrates, and oxalates. In magmatic systems, Mg is concentrated in high-temperature minerals like olivine and pyroxene.

Sodium and potassium generally come from main silicates of magmatic and clay rocks [21]. Minerals containing Na are numerous, the most common being the silicates, i.e., feldspar and Na-mica. However, Na forms a major and/or minor component of many phosphate, halide, carbonate, nitrate, borate, and sulphate minerals.

Potassium is a major constituent of many rock-forming minerals, including important silicate minerals such as alkali feldspar, leucite, biotite, muscovite, phlogopite, and some amphiboles. It is also a component of many phosphate, halide, and sulphate minerals.

Chlorides constitute approximately 0.05% of the Earth's crust and, usually, they come from rock salt dissolution or, in coastal areas, from saltwater aquifer, sea spray, and coastal flooding [21]. The main factors affecting sulphate concentration are decomposition and oxidation of substances containing sulphur (fossil fuels and dissolution of sulphur-bearing minerals such as pyrite, anhydrite, and gypsum) and human activities [15, 22]. Finally, nitrate concentration in spring water deserves particular attention because it can be a clear marker of anthropic activities affecting the aquifer (agriculture, farming, and landfilling) above all for those aquifers lying below soils without vegetation covering. Indeed, nitrate content in water bodies is the result of the balance between its input and consumption by vegetation, which plays an important role in controlling the release of nutrients [23].

The analysis of water quality finds its roots in understanding and quantifying spatially water patterns related to geological and human setting. There is thus a need to connect the information from each spring water to better understand the complex geochemical processes at a regional scale. For this reason, geostatistical methods [24] are now an essential part of the toolbox of most water scientists, who, through the spatial autocorrelation of data that creates calculated representations of spatial correlation structures, are able to study the spatial structure of spring water parameters and map their spatial distribution. Among various geostatistical methods, kriging has been defined the "BLUE," i.e., the "Best Linear Unbiased Estimator" to regionalize a variable in an unsampled location [25, 26]. Past applications of the geostatistical techniques have provided good results in investigating the relationship between the lithological nature of the aquifer and chemical composition of spring waters at a relatively small scale [27] or detecting groundwater contamination [28]. Furthermore, other studies are trying to extend the spatial groundwater analysis at a large scale [29, 30] collecting considerable amount of data and giving a precious contribution in making decision processes about water management.

The present work is the first attempt to analyse groundwater quality at a relatively large scale in the main catchment of the Calabria region (southern Italy), i.e., the Crati river basin. This area is characterized by many spring waters, and groundwater is largely used for drinking purpose, thus representing a natural and socio-economic important resource. However, few analyses on few samples have been carried out in the past years to assess the quality and the degradation processes affecting the aquifers of the Calabria region [27, 31].

The objectives of the present study were to (i) analyse the physicochemical parameters of spring water samples collected in the Crati river basin in Calabria, (ii) determine their spatial distribution, and (iii) define potential spatial anomalies. The study provides baseline information about water quality for the welfare of the society that may help in future water resource planning for the area.

2. Materials and Methods

2.1. Description of the Sampling Site. The Crati, located in the NW sector of the Calabria region, is the main basin in the region both for its extension and for its artificial lakes [32]. It has a perimeter of about 320 km and an area of 2447.7 km^2 within which a wide hydrographical network flows, including waters coming from different geological environments. The main river length is 95 km; it rises upon the Sila Massif and flows into the Ionian Sea. The average and maximum altitudes of the basin are 597 m a.s.l. and 2258 m a.s.l., respectively (Figure 1). The basin is L-shaped and can be divided into a N-S-oriented Crati and an E-W-oriented Sibari subbasins [33].

The Crati basin presents a high climatic variability owing to its position in the Mediterranean area and the mountainous nature, denoting a subtropical Mediterranean climate [34]. Specifically, on the eastern sector, high temperatures and short and heavy rainfall are observed due to the warm

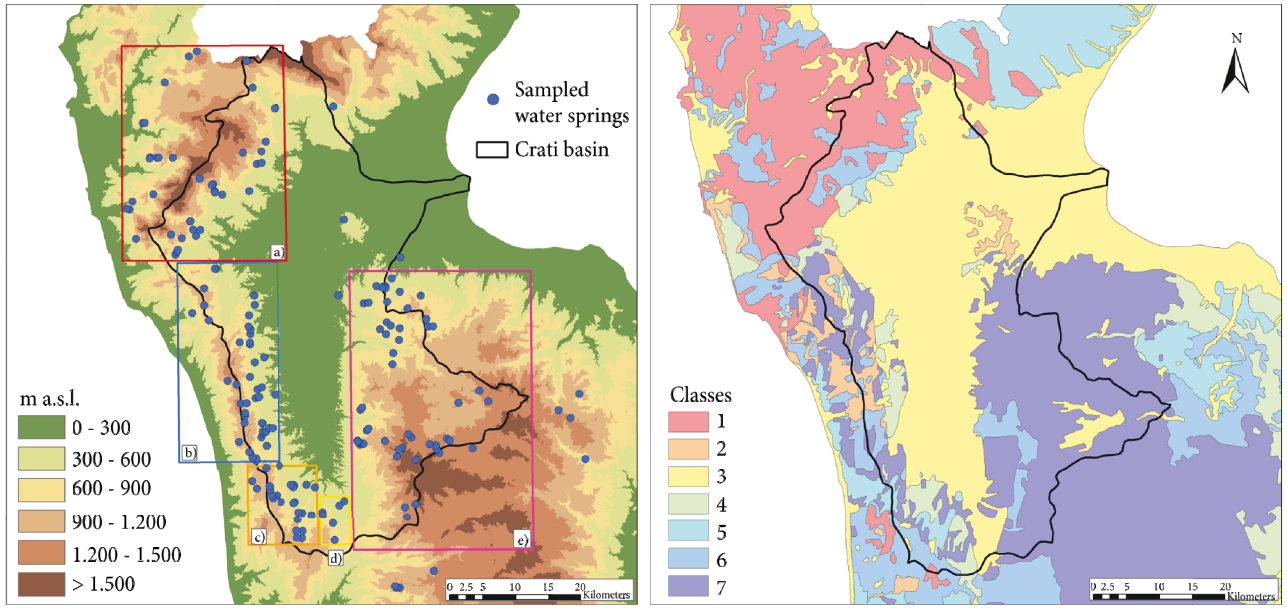

FIGURE 1: (a) Crati river basin with spring location and subzones delimited in this study: (A) Pollino Massif, (B) Coastal Chain, (C) Mt. Cocuzzo, (D) Serre Area, and (E) Sila Massif. (b) Lithological map of the basin. Lithological units are grouped into seven classes: (1) limestones and dolostones, (2) metamorphic rocks with ophiolites, (3) sand, clay and gravel, (4) clayely and marly terranes, (5) flysch, (6) sandstones, conglomerates and limestone banks, and (7) intrusive metamorphic complex.

African air currents, while the western air current affects the western side causing milder temperatures and orographic precipitation. The annual maximum and minimum precipitation are, respectively, 2106 mm (registered on the western side of the basin) and 596 mm (on the eastern side) with an average of 1212 mm. The inner areas present colder, sometimes snowy, winters and fresher, with some precipitation, summers [35, 36].

Geologically, the Crati basin is an intra-arc tectonic depression located in the north-western part of the Calabrian Arc, which is an arc-shaped continental fragment interposed between the Sicilian Maghrebide belts, to the south, and the Apennine edifice, to the north [37–39]. In particular, the Crati basin is a graben bounded by three morpho-structural highs: the plutonic and metamorphic crystalline rocks of the Sila Massif to the east, the crystalline and sedimentary rocks of the Coastal Chain to the west and south, and the carbonate and siliciclastic sedimentary rocks of the Pollino group to the north [40]. The study area is characterized by a sequence of pliocenic sediments among which are light brown and red sands and gravels, blue grey silty clays with silt interlayers, Pleistocene to Holocene alluvial sands and gravels, and very small outcrops of Miocene carbonate rocks [41, 42]. Sedimentary covering overlapped on a Palaeozoic intrusive-metamorphic complex formed by paragneiss, biotite schists, and grey phyllitic schists (with dominant quartz, chlorite, and muscovite), which are often affected by weathering processes [43]. Due to the particular tectonic setting of the basin controlled by NS, SW-NE, and NW-SE-trending faults [44], a great number of natural spring waters are located above the 300 m a.s.l. Most of them have a remarkable discharge and are currently used for drinking purposes.

In particular, the Sila Massif consists of three different Variscan metamorphic complexes (Gariglione, Mandatoriccio, and Bocchigliero complexes), respectively, representing high-, medium-, and low-grade metamorphic facies and of late-Variscan plutonites intruding them and forming the Sila batholith. The batholith consists of multiple intersecting, syn- and posttectonic intrusions, ranging in length from several kilometers to less than 1 km. They have heterogeneous texture and composition from gabbro to leucomonzogranite, with prevailing tonalite and granodiorite.

The Coastal Chain consists mainly of Paleozoic rocks with the presence of crystalline schists and ophiolites overlapped by layers of Triassic limestones as those found in Mt. Cocuzzo (1541 m a.s.l.), the highest peak of the Coastal Chain. In the tectonic window, the dolomites and the Triassic limestones appear in this area. These are stratified sedimentary deposits and occasionally massifs of an ancient carbonatic platform.

From the lithological point of view, the mountains of the Pollino are formed of Triassic, Jurassic, and Liassic limestone with frequent karst phenomena (caves, shelters, and sinkholes). Moreover, some areas near the coast have sandstone, clays, and Eocene marls. During the Mesozoic era, there is the formation in the marine environment of carbonate rocks, light grey and blackish dolomites and limestone. Starting from the Miocene Inferiore, during the formation of the Apennines, it is recorded, in the ophiolite unit and in the Oligo-Miocene terrigenous coverings, a compressive tectonics testified by folds and overlaps, which lead to the accumulation of Flysch.

In this site of the study, there is a spring of sulphur water known as “acqua fetente” (foul-smelling water). It is a condition where the running water contains a high amount of

hydrogen sulphide gas that escapes into the air. The $\delta^{34}S$ values of dissolved sulphate are constrained by the mixing of thermomineral waters with cold waters, both interacting with Upper Triassic carbonate-evaporite rocks, as well as occurrence of bacterial sulphate reduction. In the light of the geological and hydrogeological framework of the study area, this chemical and isotopic evidence suggests that the thermal circuit develops entirely into the Upper Triassic sedimentary sequence. The area is characterized also by the presence of the Rock Salt Mine of Lungro, where the Sibariti and the Romans even extracted salt and traded the rock salt. In the early 1900s, the business began to decline and the government decided the closure of the mine on November 3, 1976. Since 2015, the site is subjected to recovery and restoration.

2.2. Physical-Chemical Analyses. The discharge system of the analysed spring waters has a seasonal behaviour. The aquifers' recharge occurs generally in the period September-December, when rainfall reaches its maximum intensity and the discharge value of the spring increases with a lag time of about two months [31]. For this reason, the sampling procedure was carried out in the period from February 2016 to May 2016, when generally the maximum discharges have been recorded. In particular, 190 spring water samples were collected within the study area. In order to give a global overview of the physicochemical status, for each spring point one sample was collected by using high-density polyethylene (PE-HD) clean bottles with screw caps. In situ portable apparatus including a pH meter and a conductivity meter were used to determine the physical parameters (i.e., temperature, pH, and specific EC compensated at 20°C), while approved laboratory standard methods were applied to determine the chemical parameters, such as major cations (Ca^{2+}, Mg^{2+}, Na^{+}, and K^{+}) and major anions (SO_4^{2-}, Cl^{-}, and HCO_3^{-}) [45]. Specifically, the major cations were evaluated by using AAS (Atomic-Absorption-Spectroscopy) method; sulphate, chloride, and nitrate by UV Spectrophotometry; alkalinity by acidimetric titration; and hardness by using complexometric EDTA titration. A complete analytical quality control scheme was implemented with sampling and analytical duplicates. Analytical precision was calculated by the 20% analysis (in duplicate) of randomly chosen samples and was found to be within accepted the international standards (<5%).

2.3. Langelier-Ludwig Squared Diagram. Various diagrams have been developed over the years for visualization of water chemistry and they have been widely used by the researchers and practitioners. The first graphical technique has been proposed by [46] but, actually, the most popular diagrams are the Piper [47] and the Langelier-Ludwig square diagrams [48] which have been largely applied [49–52]. In particular, Langelier and Ludwig proposed a diagram in which rectangular coordinates are used representing patterns and correlations between major cations and anions for multiple samples, thus allowing to separate between Ca from Mg facies and Cl from SO_4 facies. More precisely, the so-called Langelier-Ludwig (LL) squared diagram allows the determination of what in geochemical practice is indicated as hydrochemical facies, reflecting the effects of chemical interaction with the lithotypes. The water classification is so ensured by positioning the water sample in one of the four sectors of which the LL diagram is composed:

(I) Chloride-sulphate Ca-Mg waters

(II) Chloride-sulphate alkaline waters

(III) Bicarbonate-alkaline waters

(IV) Bicarbonate Ca-Mg waters

The ion concentrations are expressed in meq/l. The alignment of the sample points into the different sectors allows the identification of possible phenomena such as mixing or evolutionary processes of water [31, 53].

2.4. Geostatistical Analysis. Spatial continuous data play a significant role in planning, risk assessment, and decision-making in environmental management [54]. Consequently, the mapping and spatial analysis requires converting the field measurements into continuous space. Thus, the values of an attribute at unsampled points need to be estimated, meaning that spatial interpolation from point data to spatial continuous data is necessary. The main application of geostatistics [55] to environmental sciences is the estimation and mapping of environmental matrix attributes in unsampled areas [56]. Geostatistics includes several methods that use kriging algorithms for estimating continuous attributes. For a detailed presentation of the theory of random functions, interested readers should refer to textbooks such as [25, 57–60], among others.

Before mapping and spatially interpreting the water physicochemical parameter concentration analysed, a log transformation was applied on the data, according to the assumption of decreasing data variability and allowing the data to conform more closely to normal distribution. In this way, the validity of the associated statistical analyses increases and the best data interpolation is provided. The log transformation is the most popular among the different types of transformations used to transform skewed data into approximately normal distributed data.

The level of spatial correlation is defined by the construction of the variogram and by the evaluation of the committed error. Experimental variogram is a plot showing how half of the squared differences between the sampled values (semivariance) changes with the distance between the point-pairs. It is typically expected to see smaller semivariances at shorter distances and then a stable semivariance (equal to global variance) at longer distances. It can be expressed as

$$\gamma(h) = \frac{1}{2N(h)} \sum_{i=1}^{N(h)} [Z(x_i) - Z(x_i + h)]^2, \quad (1)$$

where $\gamma(h)$ is the semivariance at a given distance h, $Z(x_i)$ is the value of variable Z at x_i location, and $N(h)$ is the number of pairs of sample points separated by the lag distance h.

Table 1: Maximum, minimum and mean concentration values of the water parameters in the 5 subzones.

	Pollino Massif			Coastal Chain			Mt. Cocuzzo			Serre Area			Sila Massif		
	Max	Min	Mean	Max	Min	Mean	Max	Min	Mean	Max	Min	Mean	Max	Min	Mean
pH	8.1	6.8	7.6	7.8	5.5	6.8	8.1	6.5	7.4	8.0	6.7	7.5	8.6	5.5	6.9
Cond (μS/cm)	936.0	195.0	414.3	636.0	65.7	206.0	1185.0	87.0	396.2	439.0	132.0	243.7	710.6	45.0	172.5
Hardness (°f)	49.5	10.7	23.7	34.4	1.6	9.1	46.1	2.7	19.0	21.8	5.0	12.1	33.6	1.0	7.3
Ca^{2+} (mg/l)	116.8	28.0	55.6	102.2	4.0	26.7	166.1	7.2	61.1	54.1	12.0	31.7	110.0	1.6	15.7
Mg^{2+} (mg/l)	50.5	2.4	23.4	21.7	1.2	6.0	27.9	1.3	9.1	20.2	4.9	10.1	20.5	1.0	7.7
K^{+} (mg/l)	2.4	0.0	1.2	15.3	0.0	1.7	19.5	0.0	1.9	2.4	0.8	1.6	2.9	0.0	1.4
Na^{+} (mg/l)	149.2	2.8	18.4	19.1	3.4	8.1	22.0	4.2	8.8	11.3	5.1	7.3	59.0	4.5	10.9
HCO_3^{-} (mg/l)	452.8	12.0	163.3	346.9	4.0	99.1	429.4	28.0	198.2	232.3	90.6	153.2	209.8	8.0	59.7
Cl^{-} (mg/l)	101.6	8.6	18.8	28.1	1.7	15.6	40.8	10.1	19.3	19.0	13.1	16.3	85.1	7.8	18.0
$SO_4^{=}$ (mg/l)	140.0	0.0	7.7	32.9	0.0	3.8	48.5	0.0	6.4	15.0	1.9	7.1	25.0	0.1	2.0
NO_3^{-} (mg/l)	17.8	0.2	4.1	14.5	0.0	1.4	8.8	0.0	2.5	5.2	0.0	1.2	24.0	0.0	4.4

Kriging is an optimal interpolator offering a minimum error variance. To estimate the variogram value analytically for any distance h, a theoretical function is fitted to the experimental variogram. The fitted variogram model allows building a model that captures the major spatial features of the attribute under study (water physicochemical parameter concentration in this study). The optimal model fitting will be chosen based on cross-validation, which checks the compatibility between the data and the structural model considering each data point in turn, removing it temporarily from the data set and using its neighbouring information to predict the value of the variable at its location [61]. The goodness of fit was evaluated by the mean error (ME) and the Mean Squared Deviation Ratio (MSDR). The difference between the measured and estimated values, represented by ME, proves the unbiasedness of estimate if its value should be close to 0, while the ratio between the squared errors and the kriging variance [26], represented by MSDR, should be 1 if the model for the variogram is accurate. In the present application for each subarea and for each analysed chemical parameter, four different semivariogram models (spherical, circular, exponential, and Gaussian) were applied and the one which provided the minor mean error (ME) was chosen as the best model. The fitted variogram was used to estimate water physicochemical parameters at unsampled locations using ordinary kriging. It aims to estimate a value of the random variable $Z(x)$ at a point of a region x_0 for which a variogram is known, using data in the neighbourhood $Z(x_\alpha)$ of the estimation location as

$$Z^*_{\mathrm{OK}}(x_0) = \sum_{\alpha=1}^{n(x_0)} \lambda_\alpha^{\mathrm{OK}} z(x_\alpha), \tag{2}$$

where λ_α is the ordinary kriging weights and $n(x_0)$ is the number of data closest to the location x_0 to be estimated. In particular, λ_α values must be evaluated in order to obtain an unbiased estimation and to minimize the variance.

Simulations are then run on normally distributed data, and the results are back-transformed. Back-transformation of each (co)kriging result was carried out by exponentiation to reverse

$$y(x_0) = \log Z(x_0), \tag{3}$$

where $Z(x_0)$ is the measured value at location x_0. This back-transformation provides a prediction for water physicochemical parameters expressed in original units.

All statistical and geostatistical analyses were performed by using the software package using cc.

3. Results and Discussion

Due to its extension, as well as to its geomorphological and hydrogeological properties, the investigated area was split into 5 subareas (Figure 1): (a) Pollino Massif, (b) Coastal Chain, (c) Mt. Cocuzzo, (d) Serre Area, and (e) Sila Massif, whose sampled waters showed different hydrochemical behaviour. In particular, the Mt. Cocuzzo area has been considered because of its calcareous nature, clearly different from the surroundings. The Serre Area has been also identified as an independent unit much more similar to a merging point between the organogenic limestones of the Mt. Cocuzzo unit, the sands and conglomerates of the graben of the Crati valley, and the granitic acid units of the Sila Massif. Basic statistics for physicochemical parameters of spring waters sampled are reported in Table 1.

Some of the following analyses have been previously presented in Gaglioti et al. [62] but for a smaller number of sampled points.

3.1. Langelier-Ludwig Squared Diagram. As a result of the physical and chemical analysis of the 190 sampled points, the Langelier-Ludwig diagram, shown in Figure 2, was obtained. The majority of the sampled spring waters falls within the first sector and the fourth sector of the diagram, corresponding to bicarbonate alkaline-earth waters and chloride-sulphate alkaline-earth waters, respectively. This result reflects very well the global lithological environment of the study area, which is mainly constituted of

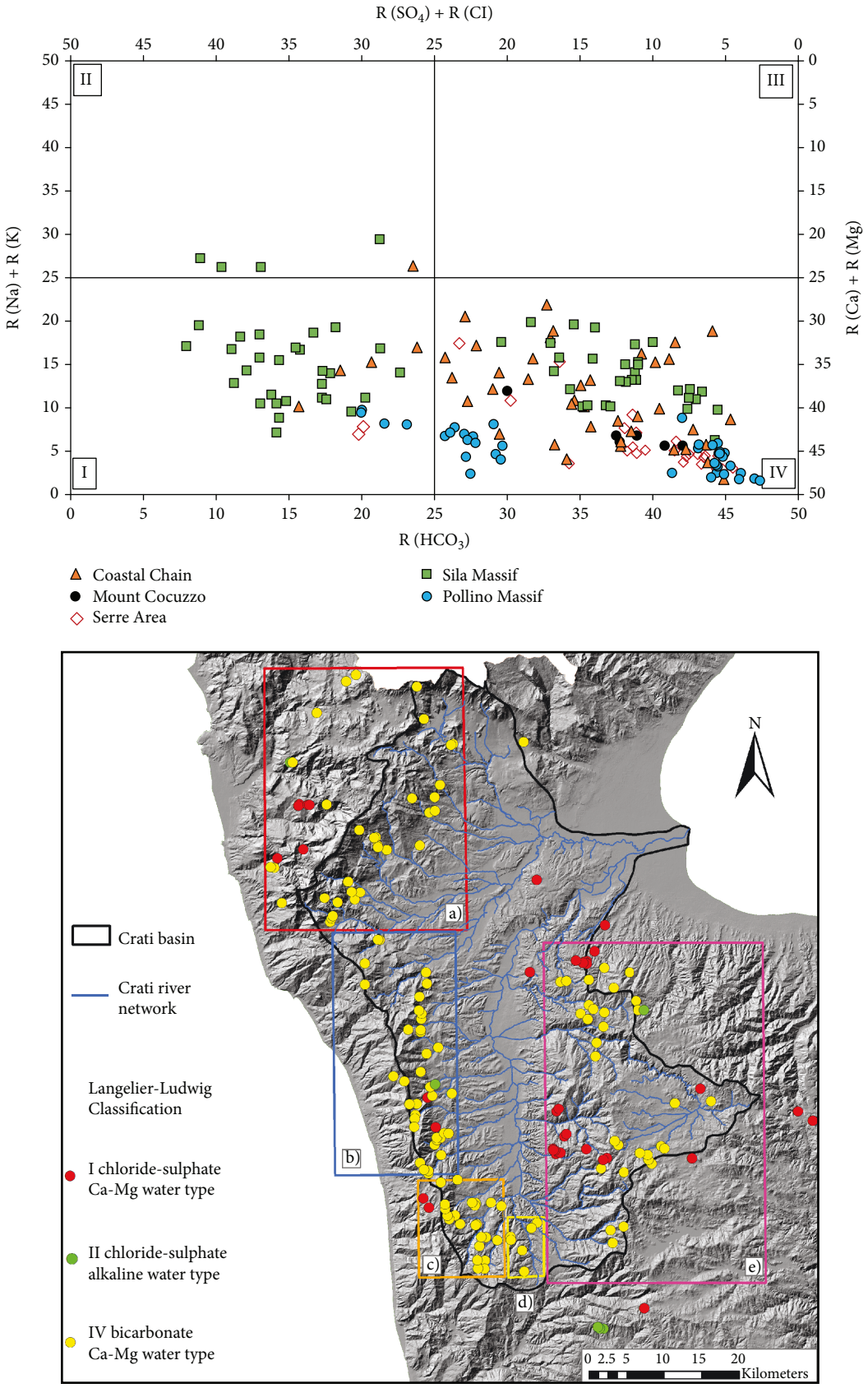

Figure 2: Langelier-Ludwig squared diagram for each area and spatial distribution of the spring water geochemical facies.

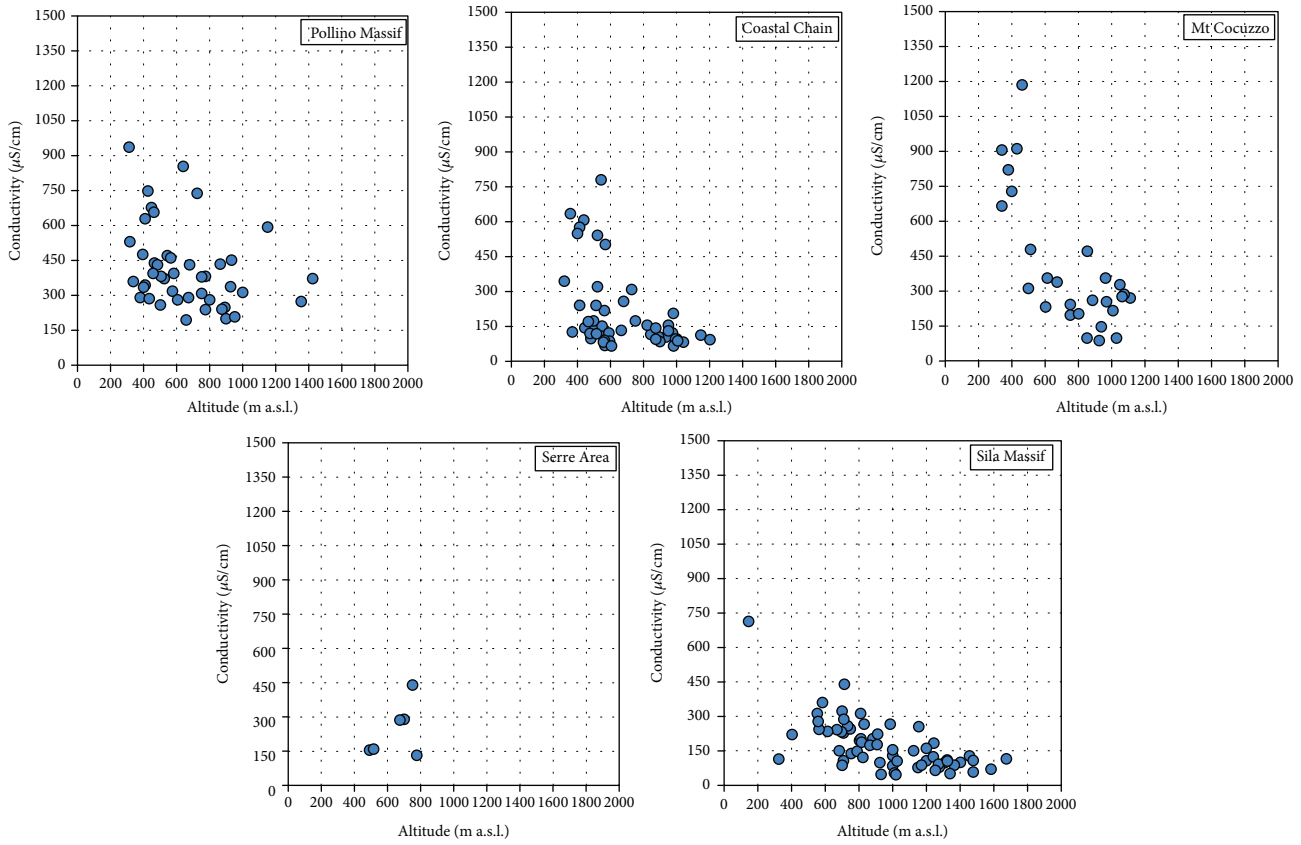

Figure 3: Relationship between spring water EC and elevation.

calcareous and carbonatic rocks (providing high Ca^{2+}, Mg^{2+}, and HCO_3^- ion concentration in water) and intrusive magmatic or metamorphic rocks (providing high SO_4^{2-}, Cl^- ion concentration in water). In particular, considering the Pollino Massif, the highest number of the samples has been identified in the fourth sector, due to hard waters particularly rich in bicarbonates, calcium, and magnesium. Moreover, these samples can be divided in two different groups, the first one very close to the lower right vertex representative of springs having low elevation, while the second group, bordering on the first sector, represents springs less conductive and thus with low mineralisation, with much more high elevation. The Coastal Chain sampled waters fall also within the fourth sector. Their position within the diagram is a little higher than those of the Pollino Massif and shows a casual distribution representative of the chemical and physical characteristic variability imputable to a mixing effect between different water types [31]. Usually, the groundwater flowing in strongly faulted areas has this behaviour [63]. In the Mt. Cocuzzo area, the results showed homogeneously grouped samples localized in the fourth sector. The lithology of this area, defined as a tectonic window, is very similar to those of the Pollino Massif, with the same calcareous origin and similar hydrochemistry. In fact, results of the analysed samples evidenced waters coming from deep aquifer, with high levels of calcium and magnesium and high alkalinity and pH values. These values are typical in carbonate aquifers. Only few spring waters differ from the others showing high sulphate content, evidencing a good correspondence with the chalky bedrock, which can be found in a very restricted area of Mt. Cocuzzo. As regards the Serre Area, the physical and chemical parameters of the sampled spring waters showed a peculiar behaviour, which differs from the neighbouring basic water of Mt. Cocuzzo and the acid ones found in the Sila Massif. Unfortunately, few numbers of sampled points did not allow getting further conclusions. Finally, from the analysis of points of the Sila Massif the water samples are located in the first sector and the fourth sector of the LL diagram, where water rich in sodium and potassium and, at the same time, poor in calcium, magnesium, and alkalinity is represented. Flowing into acid intrusive magmatic or plutonic rocks, this aquifer provides to make the water particularly acid.

3.2. Relationship between Spring Water Conductivity and Elevation. Figure 3 shows the results of the comparison between EC and altitude. This analysis allows putting in evidence some aquifer behaviour and to detect their interaction with some external factors.

For the Pollino Massif area, an almost homogeneous behaviour was identified, thus evidencing no significant trends in the diagram. In fact, limestones and dolostones make water more conductive but the depth of the aquifers, flowing in a system through rocks affected by karst phenomena, does not allow a remarkable interaction with external precipitation.

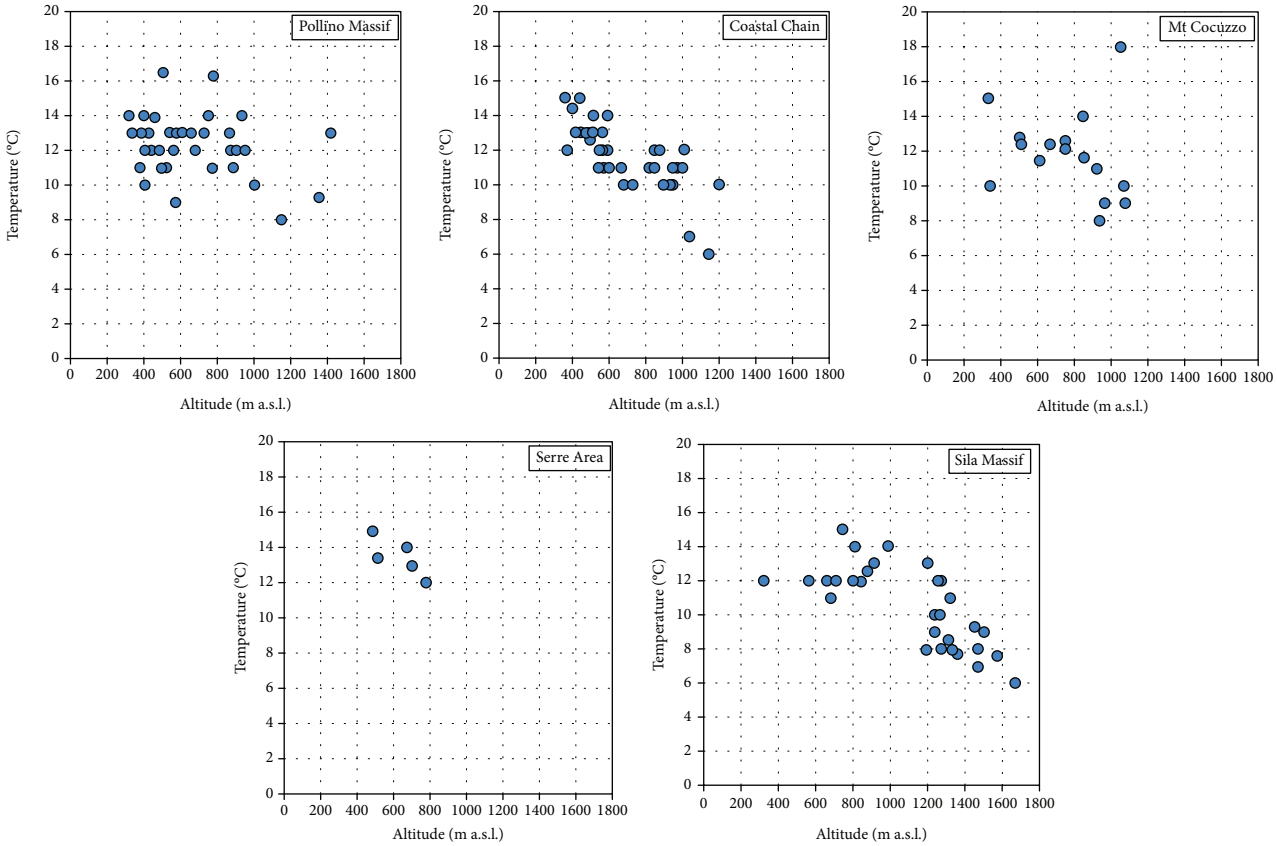

Figure 4: Relationship between spring water temperature and elevation.

In the Coastal Chain, a slight downward behaviour of the conductivity with the elevation was detected. Moreover, three different spring water groups, which should be individually studied, were identified, probably due to the presence of several aquifers at different depths.

The maximum conductivity value in all the study area (1185 μS/cm) has been detected in the Mt. Cocuzzo area, which evidenced a high variability of the conductivity with the elevation. Moreover, in this area, given the different conductivity values, two distinct spring water groups can be clearly identified. In particular, the group with high conductivity values is located on a sulphurous-chalk lithological bedrock.

In the Serre Area, no relation between spring water conductivity and elevation was evidenced.

The most interesting results have been detected in the Sila Massif, which is the area with the highest spring water altitude (1674 m a.s.l.). In fact, in this area, the lowest conductivity value (45 μS/cm) was found, thus revealing the possible presence of shallow aquifers usually influenced by rainfall [64] and infiltration into the soil. Moreover, the increase of water mineralization with altitude is strongly dependent on water-rock interaction and over time the contact. In fact, waters that infiltrate in altitude have a long route inside the aquifer (emerging at lower levels) with a consequent increase of the amount of dissolved salts transported in solution which leads to high conductive values in the spring waters at the lowest altitude. These results suggest that high-elevation springs have low solute concentration similar to those of precipitation. By contrast, due to a long time contact, lower-elevation springs are geochemically more evolved than the high-elevation springs [65].

3.3. Relationship between Spring Water Temperature and Elevation. By a visual inspection of diagrams, comparing temperature and elevation of the spring waters (Figure 4), further information can be derived. In fact, temperature can be used as a tracer of hydrologic and flowing processes for natural spring waters. Moreover, measuring the temperature accurately in field is easy, quick, and inexpensive and it also provides an insight of the subsurface geological processes. Many factors influence the spring water temperature, such as the period of the survey, the latitude, and the elevation, although the influence of the elevation is strictly dependent from the depth of the aquifer. Air temperature, solar radiation, and geothermal gradient can be considered other influencing factors on spring water temperature [66].

In the Pollino Massif and Mt. Cocuzzo areas, the sampled spring waters showed a certain homogeneity of temperature variation with the altitude, with a thermal gradient of -0.0018 and -0.0020°C/m, respectively. These features are clear sign of aquifers, which are slightly affected by the outside temperature and which, in function of their depth, maintain a certain temperature regularity evident at the spring.

Conversely, the other areas evidenced a marked reduction of the spring water temperature with elevation, thus

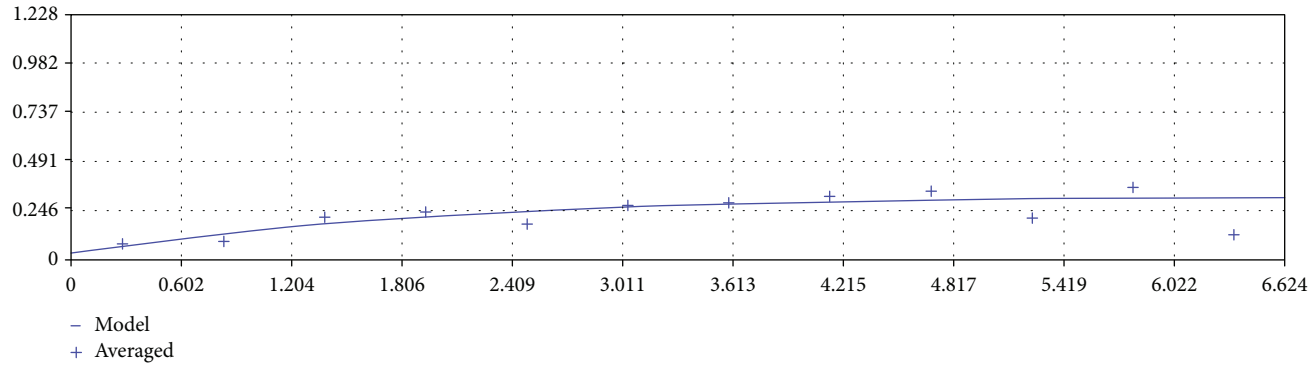

Figure 5: Experimental variogram (plotted points) and fitted model (solid line) of the calcium values in the spring waters of Mt. Cocuzzo.

denoting superficial aquifers in which water temperature is affected by air temperature. In these areas three different spring water thermal gradients with the altitude were detected, -0.0056, -0.0067, and -0.0052°C/m, respectively, which are quite similar to the annual average atmospheric gradient of the Crati valley of about -0.0068°C/m [67].

3.4. Maps of Physicochemical Parameter Spatial Distribution. To fit the shape of the experimental variogram, for each analysed parameter, four basic structures were tested including a Circular model (Cir), a Spherical model (Sph), an Exponential model (Exp), and a Gaussian model (Gau). Figure 5 shows (as an example) the variogram for calcium values in the spring waters of Mt. Cocuzzo.

The goodness of fit was checked by cross-validation and the results were quite satisfactory because the statistics used, i.e., mean of the raw estimation errors, were close to 0, while the variance of the standardized error was close to 1 (Table 2). Consequently, the best model, obtained comparing the results of ME and MSDR, was chosen to map the distribution of physicochemical parameters.

In order to obtain an instant evaluation of the main hydrogeochemical characteristics of the Crati river basin, ten thematic maps were produced, each representing the spatial distribution of the different chemical and physical parameters, making easy the identification of maximum and minimum values within the five subareas (Figures 6–8).

The maps were obtained using the ordinary kriging technique. Considering the particular distribution of the spring points, placed on average above a certain altitude, it was chosen to represent the spatial distribution maps by setting the computation process above 300 m a.s.l. The results were represented using the digital terrain model in background.

The Ca^{2+} ion is one of the most important constituents of groundwater (Figure 6). In the distribution map, the higher calcium concentrations are indicated with the most intense colours while lighter colours show areas with less concentration. By a first observation, it can be noticed that the major concentrations were found on the Pollino Massif and Mt. Cocuzzo area (in this latter case in a strictly circumscribed area); in both cases, the results agree well with the lithologic formations present, mostly of calcareous-dolomite type. On the Coastal Chain, a progressive calcium enrichment is observed, descending along the east side of the mountains, while the concentrations remain very low on the Sila Massif, both in agreement with the local geology.

The distribution map of the magnesium shows high concentrations in the northern area of the basin, where from a geological point of view, there are dolomites or rocks particularly rich in magnesium salts. On the other areas, concentrations are kept lower, ranging from 5 to 20 mg/l (Figure 6).

Observing the distribution of sodium is possible to find a particular enrichment in the Sila Massif, moving northward, whereas more restricted areas have been located in the Mt. Cocuzzo area and on the Pollino Massif where some salt mine were historically present (Figure 6).

The distribution of potassium remains fairly homogeneous throughout the basin except for the Coastal Chain where a general enrichment was recorded, descending along the slope. This behaviour is attributable to the lithological variation of the area where an important very active fault system persists that causes a "mixing" effect between waters in contact with lithologies of different nature. Also in the Serre Area, where an ancient lake basin laid, high potassium concentration was found (Figure 6).

The map of the chlorides shows the smallest concentrations on the highest altitudes of the investigated areas and gradually enriching downstream into the basin, most likely due to the different atmospheric depositions that insist on the study area. The highest concentrations were found in the Coastal Chain most likely for the residual contributions resulting from the orographic rainfall, which transport some sea aerosols, and from water-rock interaction along groundwater path (Figure 7).

Sulphate ion can be instead attributed to different origins. An exogenous nature attributable, for example, to the transport by atmospheric deposition and marine aerosols (obviously in areas near the sea) can be considered as well as in most of the cases in the present study, endogenous one. Moreover, sulphate ion can come from the dissolution of gypsum and anhydrite as in the case of the Pollino Massif, or anthropogenic input when it is together with NO_3, or due to the presence of ancient sulphur spring waters as found in the Mt. Cocuzzo area (Figure 7).

The nitrate distribution aroused a particular interest: this parameter is often indicative of the presence of intense

Table 2: Results of the cross-validation for the different subzones and the different variables.

Subzones	Variable	Model	ME	MSDR
Pollino Massif	Calcium	Circular	-0.025	0.940
	Magnesium	Exponential	-0.020	0.963
	Sodium	Spherical	-0.013	1.092
	Potassium	Gaussian	0.001	0.786
	Chloride	Exponential	-0.017	1.078
	Sulphate	Exponential	-0.065	1.009
	Nitrate	Exponential	0.015	0.945
	Alkalinity	Gaussian	-0.016	1.249
	Hardness	Exponential	0.018	0.866
	Conductivity	Spherical	-0.017	0.947
Coastal Chain	Calcium	Gaussian	-0.049	1.214
	Magnesium	Gaussian	-0.106	1.440
	Sodium	Gaussian	-0.048	0.920
	Potassium	Gaussian	-0.033	1.224
	Chloride	Gaussian	0.000	0.812
	Sulphate	Exponential	-0.060	1.583
	Nitrate	Spherical	-0.117	1.381
	Alkalinity	Exponential	-0.083	1.062
	Hardness	Circular	-0.068	1.327
	Conductivity	Exponential	-0.109	1.266
Mt. Cocuzzo	Calcium	Exponential	0.021	0.784
	Magnesium	Exponential	-0.002	1.100
	Sodium	Circular	0.024	0.941
	Potassium	Exponential	0.017	0.984
	Chloride	Gaussian	0.009	0.857
	Sulphate	Gaussian	0.052	0.875
	Nitrate	Exponential	0.008	0.959
	Alkalinity	Gaussian	-0.011	1.015
	Hardness	Circular	0.007	0.775
	Conductivity	Gaussian	0.000	1.044
Serre Area	Calcium	Gaussian	-0.016	0.505
	Magnesium	Gaussian	-0.022	0.222
	Sodium	Exponential	-0.006	1.221
	Potassium	Gaussian	-0.017	0.385
	Chloride	Gaussian	-0.035	0.536
	Sulphate	Gaussian	-0.023	0.201
	Nitrate	Gaussian	0.036	0.484
	Alkalinity	Gaussian	-0.022	0.152
	Hardness	Circular	0.076	0.977
	Conductivity	Gaussian	-0.023	0.150
Sila Massif	Calcium	Exponential	-0.041	1.045
	Magnesium	Exponential	-0.027	1.082
	Sodium	Exponential	-0.013	1.079
	Potassium	Gaussian	0.022	1.050
	Chloride	Circular	0.001	1.071
	Sulphate	Gaussian	0.008	1.019
	Nitrate	Gaussian	0.033	0.891
	Alkalinity	Exponential	-0.035	0.996
	Hardness	Exponential	-0.019	1.222
	Conductivity	Gaussian	0.017	1.086

anthropic activities, in particular farming and breeding activity, which are widespread on the Pollino Massif and Sila Massif areas. In that latter case, it has to be underlined the subsequent reforestations since the postwar period and the related cleaning and maintenance activities of the woods that have deprived the subsoil of that organic substrate necessary for denitrifying bacterial colonies (Figure 7).

Alkalinity shows high concentrations in those areas where carbonatic rocks occur, such as Pollino Massif with a quite homogeneous distribution and Mt. Cocuzzo area, where high alkalinity levels were detected in a certain localized area. The very low interaction was confirmed, in terms of carbonates and bicarbonates dissolved, for crystalline and siliceous rocks localized on the Sila Massif (Figure 7).

The map of hardness distribution, here expressed in French degrees ($1^{\circ}F = 10\,mg/l = 10\,mg\,kg^{-1}$), that is the sum of the calcium and magnesium hardness, still highlights the presence of very hard waters between the Pollino Massif and the Mt. Cocuzzo area with maximum values of 50°F for waters flowing into limestone, dolostone, and evaporitic rocks. While on the Coastal Chain and the Sila Massif the results showed the presence of soft water, mostly coming from igneous and siliceous rocks (Figure 8).

The last map (Figure 8) represents the distribution of EC, the physical parameter that synthesizes the sum of all ionic species dissolved in the water. Specifically, it is currently used in geochemistry as an indicator of the level of the so-called "maturity" of groundwaters and their flow direction. The samples with higher conductivity were found on the Pollino Massif and Mt. Cocuzzo area (849 μS/cm and 1185 μS/cm, respectively) demonstrating the presence of deep aquifers with a long-time contact with carbonatic rocks. In the Coastal Chain, a progressive enrichment was detected descending along the slope towards the east side of the basin. Relatively less conductive waters were found in the remaining areas where shallow aquifers are assumed to be present with a lower interaction with the rock substrate.

4. Conclusions

The present study is an attempt in the Crati river basin for the evaluation of the water quality of some spring waters, largely used for drinking purposes by the population. The investigation was carried out by analysing 190 spring waters all localized above 300 m a.s.l., allowing a first classification of the hydrochemical facies of the aquifers from which the same springs rise. In particular, following a preliminary analysis based on the geological characteristics of the Crati basin, the entire study area was divided into five subareas (Pollino Massif, Coastal Chain, Mt. Cocuzzo, Serre Area, and Sila Massif).

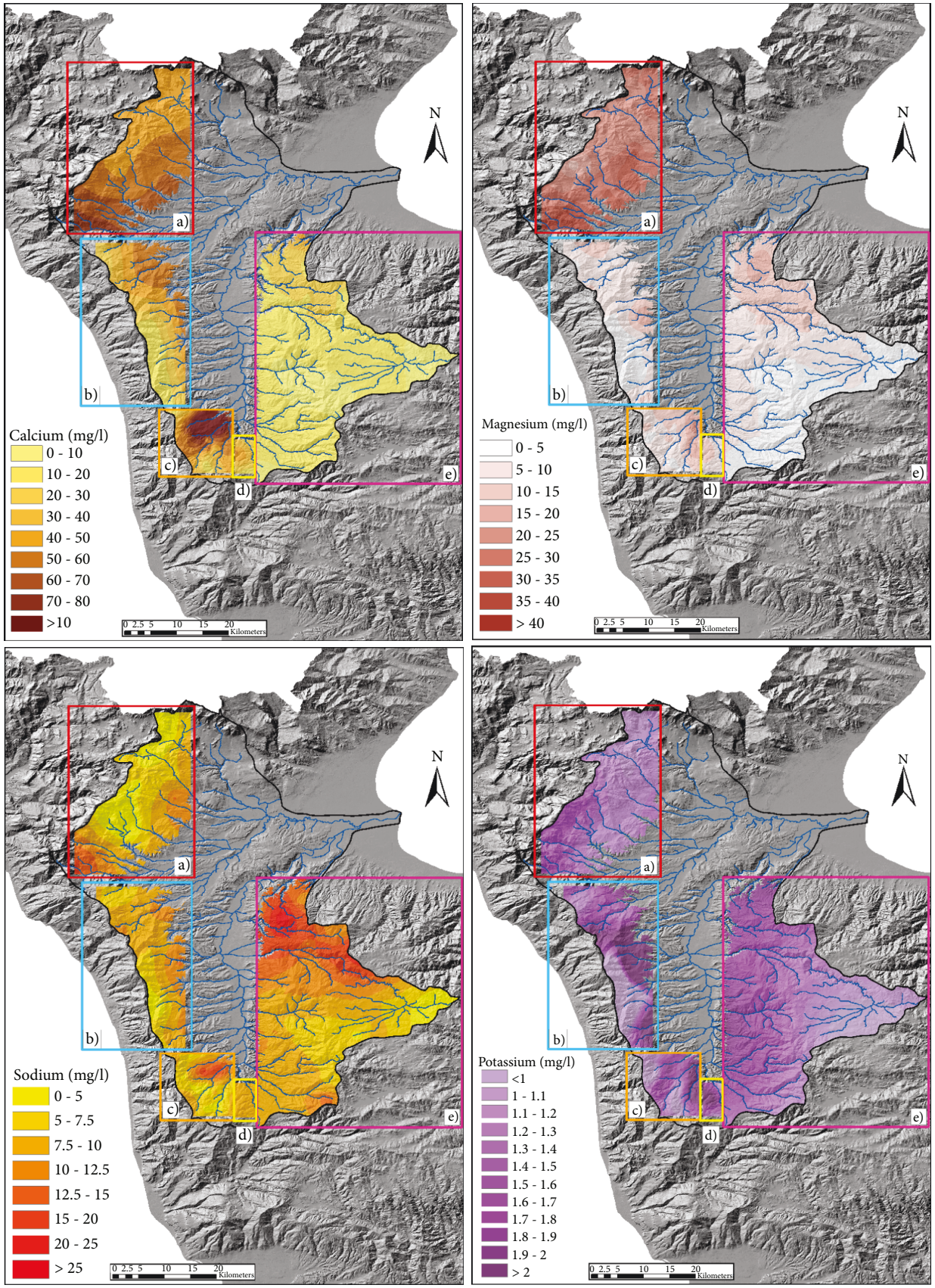

FIGURE 6: Spatial distribution of concentration of calcium, magnesium, sodium and potassium in waters from the 5 subareas of the Crati river basin.

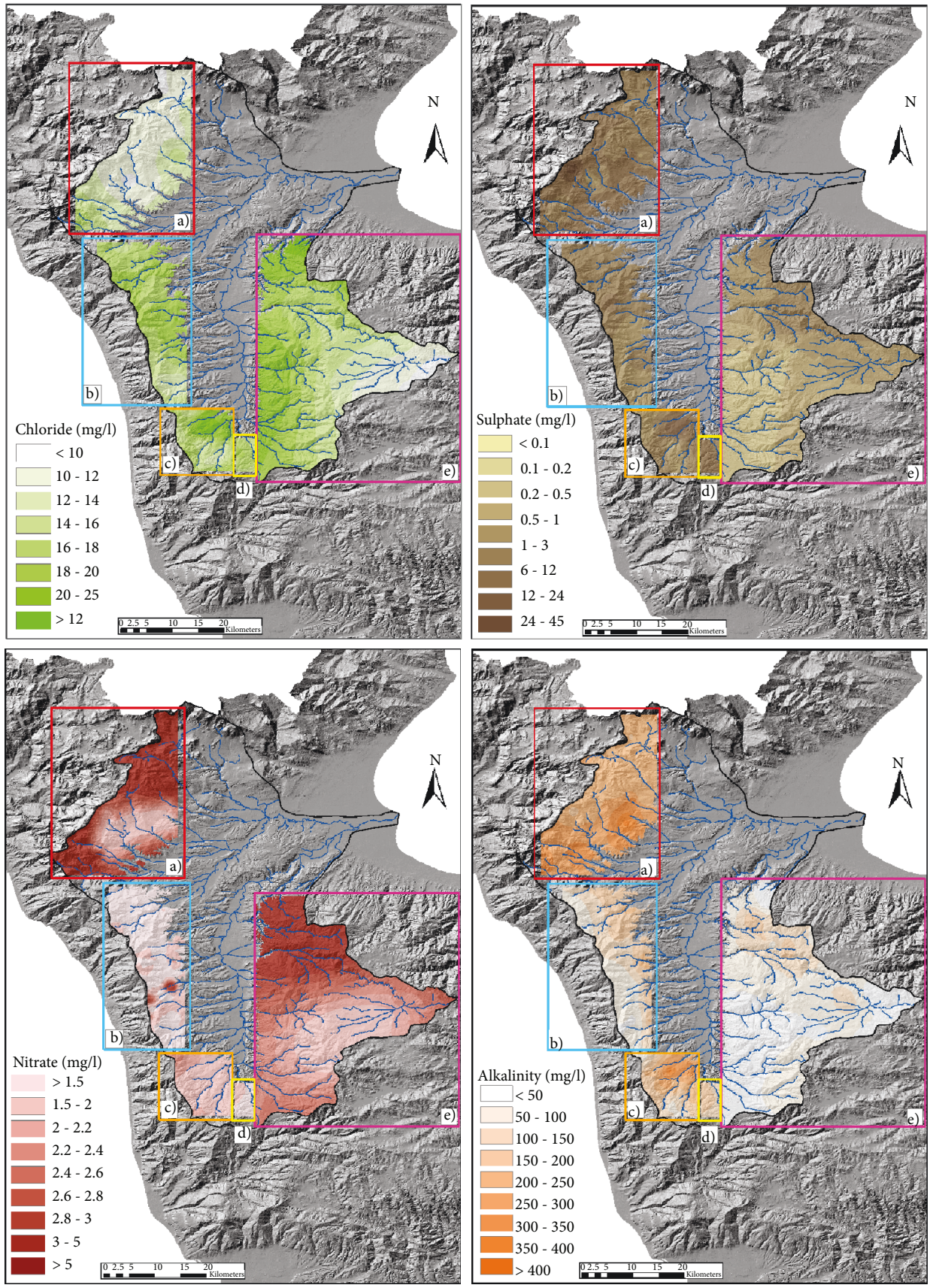

Figure 7: Spatial distribution of chloride, sulphate, nitrate and alkalinity in waters from the 5 subareas of the Crati river basin.

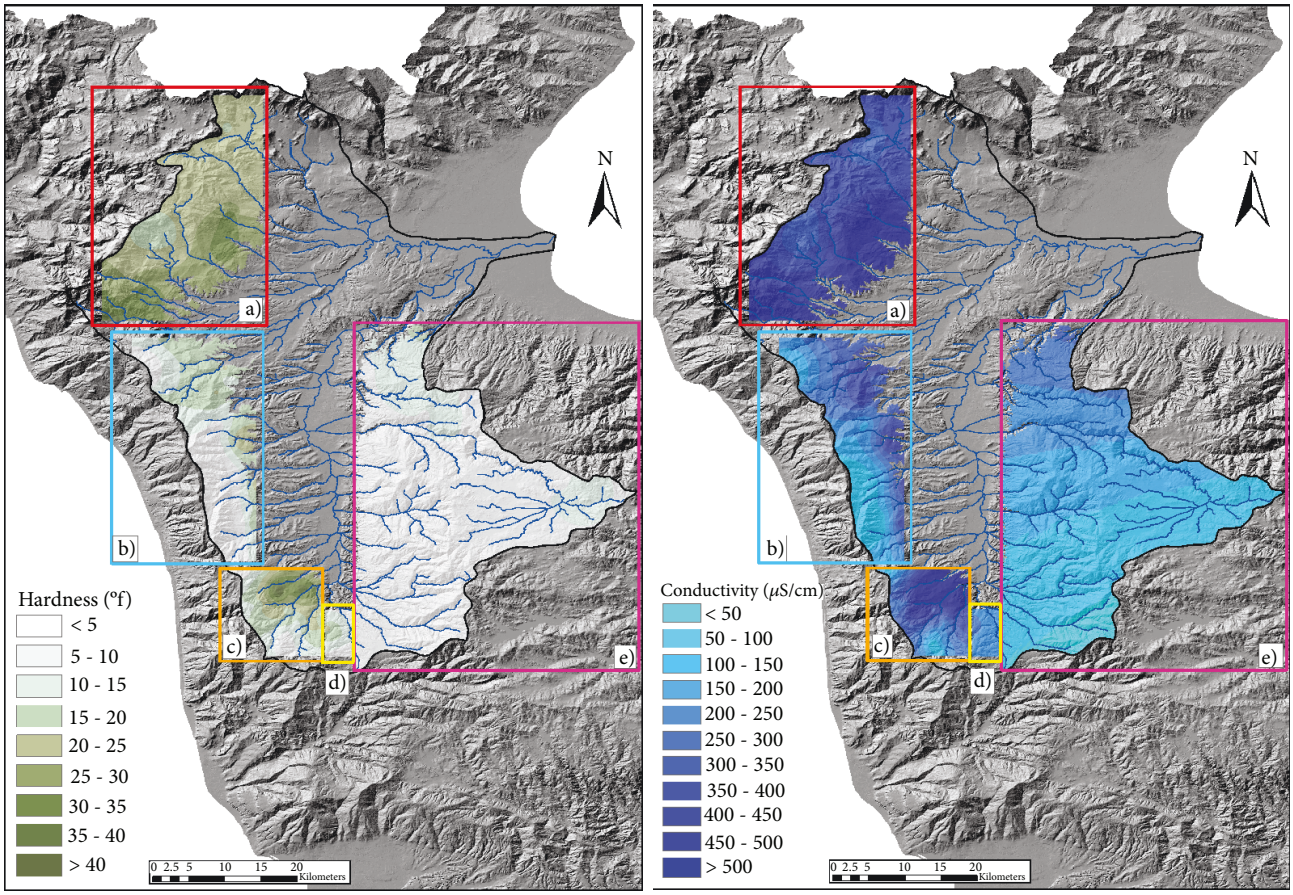

Figure 8: Spatial distribution of hardness and conductivity in waters from the 5 subareas of the Crati river basin.

As a result, the most representative water types are the bicarbonate alkaline-earth and the chloride-sulphate alkaline-earth, and only in few cases, chloride-sulphate alkaline type occur. Furthermore, the occurrence of the bicarbonate alkaline-earth water types is recorded at the highest elevations, very close to the basin borders. In particular, on the Pollino Massif and in the Mt. Cocuzzo area, very hard and alkaline waters with high conductivity and low acidity have been found. Moreover, low floating temperature values have been detected, thus evidencing waters circulating into deep calcareous aquifers having long-time contact with limestone, dolostone, and evaporitic rocks. In the Coastal Chain, a much variable behaviour in terms of dissolved salt content, conductivity, and pH levels was detected. This is probably due to the lithologic heterogeneity of the area and the presence of an important active fault system, which allows contact between lithological units with different chemical-physical characteristics. In the Sila Massif, a more homogeneous behaviour was observed, with softer water, low pH values, and low conductivity and temperature values that show a substantial downward trend as the altitude increases. These characteristics are typical of relatively shallow waters, coming from intrusive aquifers such as the granitoids and siliceous formations typical of the area.

From the observation of the distribution maps, some issues have been highlighted:

(i) In the Mt. Cocuzzo area, there is a group of spring waters showing high concentrations for almost all the investigated parameters, probably due to the process of dissolution occurring in the presence of a sulphurous-chalk lithological bedrock

(ii) In the Sila Massif, a general enrichment of the dissolved salts moving towards the north-eastern areas has been identified. An exception has been represented by nitrates, which showed high concentrations. These results are mainly due to the agriculture and the breeding activities in the area and secondly to the massive reforestation made after the Second World War and the subsequent seasonal maintenance which did not allow the natural supplying of organic substrate necessary for denitrifying bacterial colonies

(iii) Despite the little number of sampled spring waters, the Serre Area has been identified as a merging point with its intermediate lithological characteristics between the organogenic limestones of the Mt. Cocuzzo unit, the Crati graben sands and conglomerates, and Sila Massif granitic units

(iv) As concerns the Coastal Chain area, the maps confirm the presence of different lithological units that

give a noticeable water enrichment for almost all the investigated parameters descending along the east side slope of the basin

(v) The Pollino Massif area shows the highest values, homogenous distributed, in term of dissolved salts and EC

Data Availability

The data used to support the findings of this study are available from the corresponding author upon request.

Conflicts of Interest

The authors declare that they have no conflicts of interest.

References

[1] WHO, "Guidelines for drinking water quality," in *Health Criteria and other supporting information*, vol. 2, World Health Organization, Geneva, 2004.

[2] G. Pellicone, T. Caloiero, G. Modica, and I. Guagliardi, "Application of several spatial interpolation techniques to monthly rainfall data in the Calabria region (southern Italy)," *International Journal of Climatology*, vol. 38, no. 9, pp. 3651–3666, 2018.

[3] S. Dixit, S. K. Gupta, and S. Tiwari, "Nutrients overloading of a freshwater lake in Bhopal, India," *Electronic Green Journal*, vol. 21, pp. 2–6, 2005.

[4] S. K. Nag and S. Das, "Quality assessment of groundwater with special emphasis on irrigation and domestic suitability in Suri I & II Blocks, Birbhum District, West Bengal, India," *American Journal of Water Resources*, vol. 2, no. 4, pp. 81–98, 2014.

[5] D. A. Shigut, G. Liknew, D. D. Irge, and T. Ahmad, "Assessment of physico-chemical quality of borehole and spring water sources supplied to Robe Town, Oromia region, Ethiopia," *Applied Water Science*, vol. 7, no. 1, pp. 155–164, 2017.

[6] P. A. Domenico, *Concepts and Models in Groundwater Hydrology*, McGraw-Hill, New York, NY, USA, 1972.

[7] W. M. Schuh, D. L. Klinekebiel, J. C. Gardner, and R. F. Meyar, "Tracer and nitrate movement to groundwater in the Northern Great Plains," *Journal of Environmental Quality*, vol. 26, no. 5, pp. 1335–1347, 1997.

[8] S. K. Singh, M. M. Sarin, and C. France-Lanord, "Chemical erosion in the eastern Himalaya: major ion composition of the Brahmaputra and $\delta^{13}C$ of dissolved inorganic carbon," *Geochimica et Cosmochimica Acta*, vol. 69, pp. 3573–3588, 2000.

[9] S. Krishna Kumar, N. Chandrasekar, P. Seralathan, S. Prince, and N. S. M. Godson, "Hydrogeochemical study of shallow carbonate aquifers, Rameswaram Island, India," *Environmental Monitoring and Assessment*, vol. 184, no. 7, pp. 4127–4138, 2012.

[10] P. E. Potter, "Petrology and chemistry of modern big river sands," *The Journal of Geology*, vol. 86, no. 4, pp. 423–449, 1978.

[11] A. Karim and J. Veizer, "Weathering processes in the Indus River Basin: implications from riverine carbon, sulfur, oxygen, and strontium isotopes," *Chemical Geology*, vol. 170, no. 1-4, pp. 153–177, 2000.

[12] J. Quade, N. English, and P. G. Decelles, "Silicate versus carbonate weathering in the Himalaya: a comparison of the Arun and Seti River watersheds," *Chemical Geology*, vol. 202, no. 3-4, pp. 275–296, 2003.

[13] P. S. Datta and S. K. Tyagi, "Major ion chemistry of groundwater in Delhi area: chemical weathering processes and groundwater flow regime," *Journal of the Geological Society of India*, vol. 47, pp. 179–188, 1996.

[14] W. J. Deutsch, *Groundwater Geochemistry: Fundamentals and Application to Contamination*, CRC, Boca Raton, FL, USA, 1997.

[15] C. A. J. Appelo and D. Postma, *Geochemistry, Groundwater and Pollution*, Balkema Publishers, Rotterdam, 2005.

[16] W. Y. Fantong, H. Satake, S. N. Ayonghe, F. T. Aka, and K. Asai, "Hydrogeochemical controls and usability of groundwater in the semi-arid Mayo Tsanaga River Basin: Far North Province, Cameroon," *Environmental Geology*, vol. 58, no. 6, pp. 1281–1293, 2009.

[17] T. Subramani, N. Rajmohan, and L. Elango, "Groundwater geochemistry and identification of hydrogeochemical processes in a hard rock region, Southern India," *Environmental Monitoring and Assessment*, vol. 162, no. 1-4, pp. 123–137, 2010.

[18] G. Jeelani, N. A. Bhat, K. Shivanna, and M. Y. Bhat, "Geochemical characterization of surface water and spring water in SE Kashmir Valley, western Himalaya: implications to water–rock interaction," *Journal of Earth System Science*, vol. 120, no. 5, pp. 921–932, 2011.

[19] A. A. Ako, J. Shimada, T. Hosono et al., "Spring water quality and usability in the Mount Cameroon area revealed by hydrogeochemistry," *Environmental Geochemistry and Health*, vol. 34, no. 5, pp. 615–639, 2012.

[20] B. T. Kamtchueng, W. Y. Fantong, A. Ueda et al., "Assessment of shallow groundwater in Lake Nyos catchment (Cameroon, Central-Africa): implications for hydrogeochemical controls and uses," *Environment and Earth Science*, vol. 72, no. 9, pp. 3663–3678, 2014.

[21] E. Merian, M. Anke, M. Ihnat, and M. Stoeppler, *Elements and Their Compounds in the Environment*, vol. 1, Wiley, Weinheim, 2004.

[22] A. M. Nikanorov and L. V. Brazhnikova, "Water chemical composition of rivers lakes, and wetlands," in *Types and Properties of Water*, Encyclopedia of Life Support System, Vol II, EOLSS-UNESCO, 2009.

[23] E. Infusino, G. Callegari, and N. Cantasano, "Release of nutrients into a forested catchment of southern Italy," *Rendiconti Lincei*, vol. 27, pp. 127–134, 2015.

[24] G. Matheron, "The theory of regionalised variables and its applications," in *Les Cahiers du Centre de Morphologie Mathématique de Fontainebleau*, Chateau Fontainebleau, Paris, 1971.

[25] J. P. Chilès and P. Delfiner, *Geostatistics: Modelling Spatial Uncertainty*, Wiley, New York, NY, USA, 2nd edition, 2012.

[26] R. Webster and M. A. Oliver, *Geostatistics for Environmental Scientists, Second Edition*, Wiley, Chichester, 2007.

[27] C. Apollaro, C. Artusa, C. Franco, R. de Rosa, M. Polemio, and R. Virga, "Geochemical studies of spring water belonging to the Vaccuta and Abatemarco river basins (north-western Calabria, Italy)," *Italian Journal of Engineering Geology and Environment*, vol. 2, pp. 59–75, 2006.

[28] V. Elumalai, K. Brindha, B. Sithole, and E. Lakshmanan, "Spatial interpolation methods and geostatistics for mapping

groundwater contamination in a coastal area," *Environmental Science and Pollution Research*, vol. 24, no. 12, pp. 11601–11617, 2017.

[29] B. Raco, A. Buccianti, M. Corongiu et al., "GEOBASI: the geochemical Database of Tuscany Region (Italy)," *Acque Sotterranee Italian Journal of Groundwater*, vol. 4, no. 1, pp. 7–18, 2015.

[30] W. De Vos, T. Tarvainen, R. Salminen et al., *Geochemical Atlas of Europe. Part 2. Interpretation of Geochemical Maps, Additional Tables, Figures, Maps, and Related Publications, Geological Survey of Finland*, Otamedia Oy, Espoo, 2006.

[31] N. Cantasano, F. Ietto, G. Callegari, R. Froio, and E. Infusino, "Assessment of the spring water quality in the municipal area of Chiaravalle Centrale (CZ, Italy)," *L'Acqua*, vol. 3, pp. 69–76, 2013.

[32] I. Guagliardi, N. Rovella, C. Apollaro et al., "Modelling seasonal variations of natural radioactivity in soils: a case study in southern Italy," *Journal of Earth System Science*, vol. 125, no. 8, pp. 1569–1578, 2016.

[33] A. Colella, P. L. De Boer, and S. D. Nio, "Sedimentology of a marine intermontane Pleistocene Gilbert-type fan-delta complex in the Crati Basin, Calabria, southern Italy," *Sedimentology*, vol. 34, no. 4, pp. 721–736, 1987.

[34] R. Coscarelli, R. Gaudio, and T. Caloiero, "Climatic trends: an investigation for a Calabrian basin (southern Italy)," in *Proceedings of the International Symposium the Basis of Civilization* of *Water Science?*, pp. 255–266, Wallingford, 2004IAHS Publications No. 286.

[35] T. Caloiero, B. Sirangelo, R. Coscarelli, and E. Ferrari, "An analysis of the occurrence probabilities of wet and dry periods through a stochastic monthly rainfall model," *Water*, vol. 8, no. 2, p. 39, 2016.

[36] G. Buttafuoco, T. Caloiero, N. Ricca, and I. Guagliardi, "Assessment of drought and its uncertainty in a southern Italy area (Calabria region)," *Measurement*, vol. 113, pp. 205–210, 2018.

[37] L. Amodio Morelli, G. Bonardi, V. Colonna et al., "L'Arco Calabro Peloritano nell'orogene appenninico-maghrebide," *Memorie della Societa Geologica Italiana*, vol. 17, pp. 1–60, 1976.

[38] G. Bonardi, W. Cavazza, V. Perrone, and R. Rossi, "Calabria--Peloritani terrane and northern Ionian Sea," in *Anatomy of an Orogen: The Apennines and Adjacent Mediterranean Basins*, G. Bonardi, W. Cavazza, V. Perrone, and S. Rossi, Eds., pp. 287–306, Springer, Dordrecht, 2001.

[39] G. Robustelli and F. Muto, "The Crati River Basin: geomorphological and stratigraphical data for the Plio–Quaternary evolution of northern Calabria, South Apennines, Italy," *Geologica Carpathica*, vol. 68, no. 1, pp. 68–79, 2017.

[40] I. Guagliardi, N. Rovella, C. Apollaro et al., "Effects of source rocks, soil features and climate on natural gamma radioactivity in the Crati valley (Calabria, Southern Italy)," *Chemosphere*, vol. 150, pp. 97–108, 2016.

[41] D. Fabbricatore, G. Robustelli, and F. Muto, "Facies analysis and depositional architecture of shelf-type deltas in the Crati Basin (Calabrian Arc, south Italy)," *Italian Journal of Geosciences*, vol. 133, no. 1, pp. 131–148, 2014.

[42] I. Guagliardi, N. Ricca, and D. Cicchella, "From rock to soil: geochemical pathway of elements in Cosenza and Rende area (Calabria, southern Italy)," *Rendiconti Online della Società Geologica Italiana*, vol. 38, pp. 55–58, 2016.

[43] E. Le Pera, J. Arribas, S. Critelli, and A. Tortosa, "The effects of source rocks and chemical weathering on the petrogenesis of siliciclastic sand from the Neto River (Calabria, Italy)," *Sedimentology*, vol. 48, no. 2, pp. 357–378, 2001.

[44] C. Tansi, F. Muto, S. Critelli, and G. Iovine, "Neogene-Quaternary strike-slip tectonics in the central Calabrian Arc (Southern Italy)," *Journal of Geodynamics*, vol. 43, no. 3, pp. 393–414, 2007.

[45] APHA, *Standard Methods for the Examination of Water and Wastewater*, American Public Health Association, Washington, 2002.

[46] W. D. Collins, "Graphic representation of water analyses," *Industrial and Engineering Chemistry*, vol. 15, no. 4, pp. 394–394, 1923.

[47] A. M. Piper, "A graphic procedure in the geochemical interpretation of water-analyses," *Transactions, American Geophysical Union*, vol. 25, no. 6, pp. 914–923, 1944.

[48] W. F. Langelier and H. F. Ludwig, "Graphical methods for indicating the mineral character of natural waters," *Journal American Water Works Association*, vol. 34, no. 3, pp. 335–352, 1942.

[49] P. Ravikumar, K. L. Prakash, and R. K. Somashekar, "Evaluation of water quality using geochemical modeling in the Bellary Nala Command area, Belgaum district, Karnataka State, India," *Carbonates and Evaporites*, vol. 28, no. 3, pp. 365–381, 2013.

[50] N. Subba Rao, A. Subrahmanyam, S. Ravi Kumar et al., "Geochemistry and quality of groundwater of Gummanampadu sub-basin, Guntur District, Andhra Pradesh, India," *Environmental Earth Sciences*, vol. 67, no. 5, pp. 1451–1471, 2012.

[51] W. Cao, H. Yang, C. Liu, Y. Li, and H. Bai, "Hydrogeochemical characteristics and evolution of the aquifer systems of Gonghe Basin, Northern China," *Geoscience Frontiers*, vol. 9, no. 3, pp. 907–916, 2017.

[52] N. Subba Rao, G. Vidyasagar, P. Surya Rao, and P. Bhanumurthy, "Chemistry and quality of groundwater in a coastal region of Andhra Pradesh, India," *Applied Water Science*, vol. 7, no. 1, pp. 285–294, 2017.

[53] C. Apollaro, A. Bloise, R. De Rosa et al., "Caratterizzazione idrogeochimica e qualità delle acque di un acquifero ospitato entro rocce metamorfiche nella Calabria nord occidentale," *Engineering Hydro Environmental Geology*, vol. 12, pp. 95–102, 2009.

[54] J. Li and A. Heap, "A review of spatial interpolation methods for environmental scientists," Geoscience Australia, Canberra, 2008.

[55] G. Matheron, "Principles of geostatistics," *Economic Geology*, vol. 58, no. 8, pp. 1246–1266, 1963.

[56] P. Goovaerts, "Geostatistics in soil science: state-of-the-art and perspectives," *Geoderma*, vol. 89, no. 1-2, pp. 1–45, 1999.

[57] P. Goovaerts, *Geostatistics for Natural Resources Evaluation*, Oxford University Press, New York, NY, USA, 1997.

[58] A. G. Journel and C. J. Huijbregts, *Mining Geostatistics*, Academic, San Diego, CA, USA, 1978.

[59] H. Wackernagel, *Multivariate Geostatistics: An Introduction with Applications*, Springer-Verlag, Berlin, 2003.

[60] E. H. Isaaks and R. M. Srivastava, *Applied Geostatistics*, Oxford University Press, New York, NY, USA, 1989.

[61] G. Buttafuoco, A. Tallarico, G. Falcone, and I. Guagliardi, "A geostatistical approach for mapping and uncertainty assessment of geogenic radon gas in soil in an area of southern Italy,"

Environmental Earth Sciences, vol. 61, no. 3, pp. 491–505, 2010.

[62] S. Gaglioti, E. Infusino, T. Caloiero, and G. Callegari, "Hydrochemical and qualitative assessment of natural water spring in southern Italy," *European Water*, vol. 57, pp. 399–405, 2017.

[63] L. Tortorici, "Lineamenti geologico-strutturali dell'Arco Calabro-Peloritano," *Rendiconti, Società Italiana di Mineralogia e Petrologia*, vol. 38, pp. 927–940, 1982.

[64] E. Infusino, G. Callegari, and G. Frega, "Deposizioni atmosferiche nell'area urbana di Cosenza in Calabria," in *Proceedings XXIII of the Giornata dell'ambiente 2005 "Qualità dell'aria nelle città Italiane"*, vol. 227, pp. 145–154, Accademia dei Lincei, Bardi editore, Rome, 2006.

[65] J. C. Wilcox, W. D. Holland, and J. M. Mcdougald, "Relation of elevation of a mountain stream to reaction and salt content of water and soil," *Canadian Journal of Soil Science*, vol. 37, no. 1, pp. 11–20, 1956.

[66] P. Celico, "Prospezioni geochimiche," in *Prospezioni idrogeologiche*, pp. 307–357, Liguori Editore, Napoli, 1986.

[67] G. Callegari, G. Frega, and E. Infusino, "Problemi di stabilità atmosferica. Loro influenza sulle precipitazioni - un caso di studio nella valle del F. Crati," in *Proceedings (in CD) of the International Symposium di Ingegneria Sanitaria Ambientale*, pp. 1–16, Taormina, 2004.